

Array RF Transmitter for 7T MRI of the Spine Based on Dipole Antennas

Qi Duan¹, Natalia Gudino¹, Jacco A. de Zwart¹, Peter van Gelderen¹, Joe Murphy-Boesch¹, Jeff H. Duyn¹, and Hellmut Merkle¹
¹LFMI, National Institute of Neurological Disorders and Stroke, National Institutes of Health, Bethesda, Maryland, United States

Target Audience MR physicists, engineers.

Purpose: Imaging of large objects at high field generally requires sophisticated RF coil structures to mitigate signal dropouts associated with wavelength effects. For imaging the human spine at 7T (300MHz), arrays with a certain combination of transmit and receive elements have been proposed¹⁻⁵, which generally have a complex electrical structure. Although it is possible to simplify the RF excitation by exploiting the traveling wave phenomenon (e.g. by employing a patch antenna at bore entrance⁶), this may have inferior sensitivity and undesirable RF power deposition outside the region of interest. Here we explored the feasibility of using an array of electric dipole antennas (e.g.⁷) for RF transmission in spine MRI at high field.

Methods

Two dipoles were constructed from 10 mm wide copper tape to perform quadrature excitation. Their length of 370 mm was chosen to match $\lambda/2$ at 300MHz. The conductors were connected at one end to a home-built $\lambda/8$ - $\lambda/12$ hybrid and through two home-built TR switches to preamplifiers for signal reception (Fig.1a). Performance was evaluated with a sugar-gel phantom mimicking the electrical properties of average muscle tissue ($\sigma=0.79\text{S/m}$, $\epsilon_r=59$). To evaluate the transmit efficiency, a modified Bloch-Siegert B_1^+ mapping sequence⁸ was used. All MR experiments were performed on a Siemens 7T scanner. After optimization of conductor separation under quadrature drive via MR imaging, manipulation of the B_1^+ amplitude distribution was explored by changing the phase difference between the dipoles through varying cable length. The optimal phase and spatial shift combination was then used to compare the transmit efficiency to a loop based 7T spine array² optimized via a similar approach.

Results and Discussion

B_1^+ amplitude in terms of S_{21} as a function of distance from the dipole was measured in free space under various loading conditions (Fig. 1b). Except for the unloaded case, distance dependence behaved similarly. This relative insensitivity to loading is beneficial for high field application. MR experiments showed that at 5 cm depth within the phantom, a 6 cm separation between the dipoles provided a good trade-off between transmit efficiency and inter-element coupling. The S_{11} of each dipole was < -30 dB and S_{21} was ~ -12 dB between the dipoles. The transmit efficiency as a function of phase delay between the two antennas was measured by B_1^+ mapping and is demonstrated in Fig. 2, with high noise regions masked out. The capability of “steering” the transmit field is clearly demonstrated. Based on these results, the configuration of the array was optimized with respect to phase shift between the two antennas as well as horizontal spatial shifts between the center of the array and the center of the ROI (to accommodate any potential field twisting effects²) to maximize the transmit efficiency within a 20 mm diameter ROI at 50 mm depth (see Fig.3a for 3D plot), with 142° and 9 mm shift being the optimum. Using quadrature drive for simplicity, performance remained within 97% of the optimum (Fig.3b). We compared the dipole array with a home-built 8-channel loop array with similar coverage (Fig. 4, the curved boundaries in sagittal and coronal planes were due to gradient nonlinearity). The dipole array appeared to have an at least equivalent performance than the loop array. Considering the advantage of its simplicity, the dipole array appears a promising approach that is competitive with loop designs.

Conclusion

A transmit array based on electric dipoles was built for 7T spine imaging. Field steering capability was shown in a phantom study. The transmit efficiency was compared to a previously proposed design based on quadrature loop excitation. The newly proposed antenna array provides a much simpler and more efficient design that can be combined with existing receive array technology. Similar transmit structures can be used for other applications.

Reference

1. Kraff O, Bitz AK, Kruszona S, et al. An eight-channel phased array RF coil for spine MR imaging at 7 T. *Invest Radiol*. Nov 2009;44(11):734-740.
2. Duan Q, Sodickson DK, Lattanzi R, Zhang B, Wiggins G. Optimizing 7 T spine array design through offsetting of transmit and receive elements and quadrature excitation. *18th Annual Meeting & Exhibition of ISMRM*. Vol Stockholm, Sweden 2010:324.
3. Zhao W, Cohen-Adad J, Polimeni JR, et al. Nineteen-channel receive array and four-channel transmit array coil for cervical spinal cord imaging at 7T. *Magn Reson Med*. Aug 20.
4. Sigmund EE, Suero GA, Hu C, et al. High-resolution human cervical spinal cord imaging at 7 T. *NMR Biomed*. Jul;25(7):891-899.
5. Wu B, Wang C, Krug R, et al. 7T human spine imaging arrays with adjustable inductive decoupling. *IEEE Trans Biomed Eng*. Feb;57(2):397-403.
6. Brunner DO, De Zanche N, Frohlich J, Paska J, Pruessmann KP. Travelling-wave nuclear magnetic resonance. *Nature*. Feb 19 2009;457(7232):994-998.
7. Raaijmakers AJ, Ipek O, Klomp DW, et al. Design of a radiative surface coil array element at 7 T: the single-side adapted dipole antenna. *Magn Reson Med*. Nov;66(5):1488-1497.
8. Duan Q, van Gelderen P, Duyn J. Improved Bloch-Siegert based B(1) mapping by reducing off-resonance shift. *NMR Biomed*. Jan 28 2013;26(9):1070-1078.

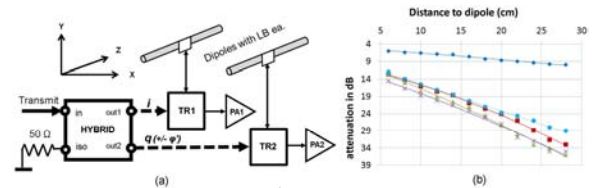


Fig. 1: (a) transmit array design (b) B_1^+ field as a function of distance. The dark blue one (top) is unloaded, the rest are with various distances to the load (13,19,26,50mm)

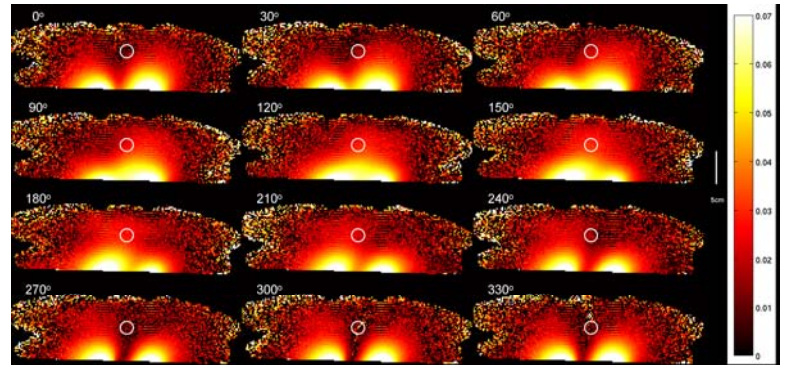


Fig. 2: Axial B_1^+ efficiency map (unit $\mu\text{T/V}$) at the center as a function of phase delay (high noised regions were masked out). White circles represent the approximate locations of spinal cord.

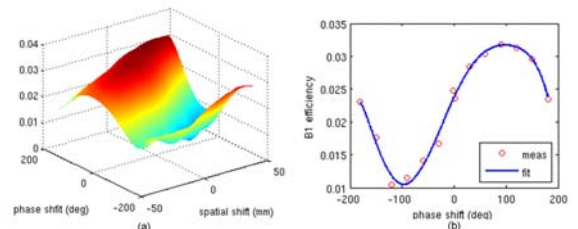


Fig. 3: B_1^+ efficiency: (a) as a function of phase shift and spatial shift; (b) measured (red dot) and fitted data (blue line) with 6th order polynomial for quadrature drive.

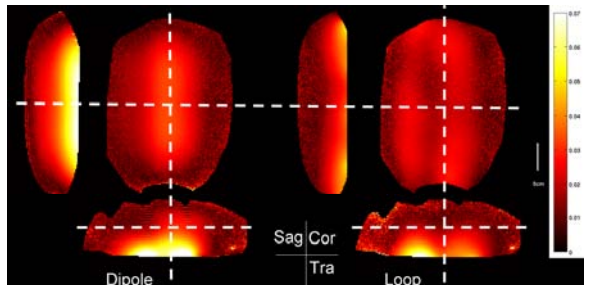


Fig. 4: Masked B_1^+ efficiency comparison in three planes. White dashed lines show approximate slice positions.